JOURNAL OF AIRCRAFT
Vol. 37, No. 3, May–June 2000

Escaping Microburst with Turbulence: Altitude, Dive, and Pitch Guidance Strategies

Atilla Dogan* and Pierre T. Kabamba†
University of Michigan, Ann Arbor, Michigan 48109-2140

Three escape strategies are compared for microburst encounters during final landing approach: altitude guidance, dive guidance, and pitch guidance. The main difference between pitch guidance and the other two strategies is that pitch guidance immediately attempts to increase altitude at the expense of airspeed, whereas dive and altitude guidances initially trade altitude for airspeed. We use a full, six-degree-of-freedom, nonlinear, rigid-body aircraft model, including the effects of windshear and wind vorticity, and a model of microburst with turbulence. We also model the effect of stall prevention on the escape path. Two different approaches are used for comparison: 1) In a sample analysis approach, typical samples of the time histories of various variables are analyzed. 2) In a statistical approach, the probability distribution of the minimum altitude is estimated by the Monte Carlo method when the statistical properties of the microburst parameters are known. In the sample analysis and statistical approaches, the simulations take into account turbulence in addition to windshear. Both approaches suggest that, within the modeling assumptions presented, and in the absence of human factors, altitude and dive guidance with low commanded altitude may provide better safety than pitch guidance.

Nomenclature

b = span, m
$\bar{c}$ = chord, m
D = drag, N, or diameter of the peak radial outflow-velocity contour, m
D_θ = the set in which the parameter vector $\boldsymbol{\theta}$ assumes values
E = specific energy, m
$E[\cdot]$ = expected value of a random variable
$F_{h_{\min}}(h)$ = probability distribution function of $h_{\min}$
f_h = intensity of the downdraft, 1/s
f_r = intensity of the horizontal shear, 1/s
g = acceleration of gravity, m/s^2
h = altitude, m
$h_{\min}$ = minimum altitude reached in an escape maneuver, m
I_{xx} = moment of inertia around body x axis, kg $\cdot$m^2
I_{xz} = product of inertia on body x–z plane, kg $\cdot$m^2
I_{yy} = moment of inertia around body y axis, kg $\cdot$m^2
I_{zz} = moment of inertia around body z axis, kg $\cdot$m^2
$\boldsymbol{K}$ = control gain vector
L = lift, N; or lower bound of a confidence interval; or scale length, m
$\mathcal{L}$ = rolling moment, N $\cdot$m
$\mathcal{M}$ = pitching moment, N $\cdot$m
m = mass of the aircraft, kg
$\mathcal{N}$ = yawing moment, N $\cdot$m
p = angular velocity around body x axis, 1/s
q = angular velocity around body y axis, 1/s
r = radial distance from the microburst center, m; or angular velocity around body z axis, 1/s
S = side force, N
$\mathcal{S}$ = wing area, m^2
T = thrust, N
U = upper bound of a confidence level
u_g = components of turbulence in body x axis, m/s
V = airspeed, m/s
v_g = components of turbulence in body y axis, m/s
W = weight of the aircraft, N
$W_{(\cdot)}$ = wind velocity component in $(\cdot)$ direction, m/s
w_g = components of turbulence in body z axis, m/s
x = longitudinal distance from the runway threshold, m
x_c = location of the microburst center in x direction, m
y = lateral distance from the runway threshold, m
y_c = location of the microburst center in y direction, m
z = vertical direction into the ground, m
$\boldsymbol{z}_0$ = initial condition of the aircraft state vector
α = angle of attack, rad or deg
β = side slip angle, rad or deg
Δz = moment arm of thrust around body y axis, m
δ = confidence parameter, or thrust inclination angle, rad
δ_a = aileron deflection, rad or deg
δ_e = elevator deflection, rad or deg
δ_r = rudder deflection, rad or deg
θ = pitch angle, rad or deg
$\boldsymbol{\theta}$ = microburst parameters and turbulence vector
ξ = throttle response
ξ_t = throttle setting
ρ = air density, kg/m^3
σ = intensity of turbulence component, m/s
Φ = power spectral density function of body x-axis turbulence component, m^2/s
ϕ = bank angle, rad or deg
ψ_w = angle between the direction of radial wind and x axis, rad

Subscripts

c = commanded
rel = relative to air
u_g = body x-axis turbulence component
v_g = body y-axis turbulence component
w_g = body z-axis turbulence component

Received 7 July 1998; revision received 9 September 1999; accepted for publication 8 January 2000.

*Graduate Student, Department of Aerospace Engineering; adogan@engin.umich.edu. Student Member AIAA.
†Professor, Department of Aerospace Engineering; kabamba@engin.umich.edu.

Introduction

THIS paper studies escape maneuvers for an aircraft flying, during a final landing approach, through windshear due to a microburst. Windshear is a spatial and temporal variation of atmospheric winds that can cause an aircraft to deviate from the intended flight path. Among many atmospheric phenomena that cause windshear, the one called microburst is the most dangerous

for aircraft because of its magnitude and short life. A microburst is a small downburst with damaging wind extending only 4 km or less.[1] From 1964 to 1982, 27 U.S. aircraft accidents or incidents involving nearly 500 fatalities have been attributed to low-altitude windshear.[2] According to a report obtained from the National Transportation Safety Board (NTSB), from 1990 to 1995 there have been 11 U.S. aircraft accidents with 41 fatalities involving microburst as cause/factor/finding. Noticeably, all of the accidents occurred during landing approach, when the pilot either attempted to land through a strong microburst or initiated an escape maneuver too late.

The Federal Aviation Administration's (FAA's) Windshear Training Aid[3] recommends that, on recognizing an encounter with severe windshear, the pilot should command maximum thrust and rotate the aircraft to an initial target pitch angle of 15 deg. We refer to this strategy as pitch guidance. After the FAA's recommendation, a substantial research effort has been devoted to finding safe strategies for microburst encounters and designing controllers to implement them. In most of these papers, the goal has been to develop a feedback control law that flies the aircraft on an optimal trajectory.[4–11] The common feature of the optimal escape trajectories in most studies has been to increase or to maintain the altitude without excessive loss of kinetic energy or airspeed.[4–11] Most of the papers where uncertainties in microburst strength and size are considered study the encounter during takeoff or approach landing.[4–9,12–15] In Refs. 12–14, the equations of motion are linearized along the takeoff or landing path, and linear robust control techniques are used. In Refs. 5 and 14 the distributions of deviations of some aircraft states from their nominal values are computed by Monte Carlo simulation. In Refs. 4, 6–9, and 15, optimization problems are solved for a few microburst parameters to see the difference in trajectories through microbursts of different strength and size. In almost all papers, the flight is assumed to take place in a vertical plane. Exceptions are Refs. 10, 11, and 16, where lateral maneuvers are studied together with longitudinal maneuvers. Reference 10 introduced the commanded altitude guidance strategy as the solution of an optimization problem. The feedback law developed in Ref. 11 to implement the optimal strategy directs the aircraft, with full thrust, to a constant recovery altitude while turning the aircraft away from the microburst core. Among the microburst escape studies, only Refs. 11 and 15 suggest that initial descent may improve the safety of an escape maneuver. Reference 17 introduced the probability of crash and showed that it is decreased by initial descent. However, these papers neglect the rotational dynamics of the aircraft, the effect of turbulence and air vorticity on the escape performance, and the effect of stall prevention on the escape path.

This paper compares the following three guidance laws: pitch guidance,[3] dive guidance,[3] and altitude guidance[11] from the point of view of safety. By safety we mean that, throughout an escape maneuver, 1) the aircraft never runs into stall and 2) ground contact never occurs. In this paper, the failure of any of these two conditions will be deemed a crash. Although it is assumed that obstacle clearance is not a concern, we have experimental evidence that the results of this study still hold when altitude is constrained to remain above a low threshold. Pitch guidance is chosen as the baseline strategy in this study because it is the strategy recommended by the FAA. The main difference between pitch guidance and the other two guidance laws is that pitch guidance attempts immediately to increase altitude, whereas altitude is initially traded for airspeed in the other two strategies.

The original features of this study are as follows. We use a full, six-degree-of-freedom (DOF), nonlinear, rigid-body aircraft model, including the effects of windshear and wind vorticity, and a model of microburst with turbulence. We also model the effect of stall prevention on the escape path. Another notable original feature of this study is an estimate of the probability distribution of the minimum altitude by the Monte Carlo method, used to make a conclusive comparison between different strategies in microbursts whose properties have statistical variations and in the presence of turbulence. Our results suggest that, within the modeling assumptions of this paper, and in the absence of human factors, altitude and dive guidance with low commanded altitude may provide better safety than pitch guidance. These results are similar to those in Refs. 11 and 15, however, unlike Ref. 11 or Ref. 15, our results suggest that safety degrades when the target altitude is lower than an optimal threshold.

Mathematical Model

The full, six-DOF, nonlinear, rigid-body aircraft dynamic model, including the effects of windshear and wind vorticity, consists of the following, 13-state system of equations. This set of equations is equivalent to that given in Refs. 18 and 19. Aircraft data and aerodynamic coefficients used in this study are representative of a large, jet-engine commercial transport airplane in landing configuration.[20]

The translational dynamics are

$$\begin{aligned}\dot{V} &= g[\cos\theta\sin\beta\sin\phi + \cos\beta(\cos\phi\cos\theta\sin\alpha - \cos\alpha\sin\theta)] \\ &\quad + (1/m)[-D + T\cos(\alpha+\delta)\cos\beta] \\ &\quad - [er(1,1)\dot{W}_x + er(1,2)\dot{W}_y + er(1,3)\dot{W}_z] \end{aligned} \tag{1}$$

$$\begin{aligned}\dot{\beta} &= -r\cos\alpha + p\sin\alpha + (g/V)(-\cos\phi\cos\theta\sin\alpha\sin\beta \\ &\quad + \cos\beta\cos\theta\sin\phi + \cos\alpha\sin\beta\sin\theta) \\ &\quad - (1/mV)[S + T\cos(\alpha+\delta)\sin\beta] \\ &\quad - [er(2,1)\dot{W}_x + er(2,2)\dot{W}_y + er(2,3)\dot{W}_z] \end{aligned} \tag{2}$$

$$\begin{aligned}\dot{\alpha} &= q - (p\cos\alpha + r\sin\alpha)\tan\beta + (g\sec\beta/V)[\cos\alpha\cos\phi\cos\theta \\ &\quad + \sin\alpha\sin\theta] - (\sec\beta/mV)[L + T\sin(\alpha+\delta)] \\ &\quad - [er(3,1)\dot{W}_x + er(3,2)\dot{W}_y + er(3,3)\dot{W}_z] \end{aligned} \tag{3}$$

where

$$er = \mathcal{E}^{-1}R(\psi,\theta,\phi) \tag{4}$$

$$\mathcal{E}^{-1} = \begin{bmatrix} \cos\alpha\cos\beta & \sin\beta & \cos\beta\sin\alpha \\ -(\cos\alpha\sin\beta/V) & \cos\beta/V & -(\sin\alpha\sin\beta/V) \\ -(\sec\beta\sin\alpha/V) & 0 & \cos\alpha\sec\beta/V \end{bmatrix} \tag{5}$$

and $R(\psi,\theta,\phi)$ is the 3–2–1 rotation matrix.

The translational kinematics are

$$\begin{aligned}\dot{x} &= V[\cos\beta\cos\alpha\cos\theta\cos\psi + \sin\beta(-\cos\phi\sin\psi \\ &\quad + \sin\phi\sin\theta\cos\psi) + \cos\beta\sin\alpha(\sin\phi\sin\psi \\ &\quad + \cos\phi\sin\theta\cos\psi)] + W_x \end{aligned} \tag{6}$$

$$\begin{aligned}\dot{y} &= V[\cos\beta\cos\alpha\cos\theta\sin\psi + \sin\beta(\cos\phi\cos\psi \\ &\quad + \sin\phi\sin\theta\sin\psi) + \cos\beta\sin\alpha(-\sin\phi\cos\psi \\ &\quad + \cos\phi\sin\theta\sin\psi)] + W_y \end{aligned} \tag{7}$$

$$\begin{aligned}\dot{z} &= V[-\cos\beta\cos\alpha\sin\theta + \sin\beta\sin\phi\cos\theta \\ &\quad + \cos\beta\sin\alpha\cos\phi\cos\theta] + W_z \end{aligned} \tag{8}$$

The rotational dynamics are

$$\begin{aligned}\dot{p} &= \left[1\Big| \left(I_{xx}I_{zz} - I_{xz}^2\right)\right]\left[(I_{xx} - I_{yy} + I_{zz})I_{xz}pq \right. \\ &\quad \left. + \left(I_{yy}I_{zz} - I_{zz}^2 - I_{xz}^2\right)qr + I_{zz}\mathcal{L} + I_{xz}\mathcal{N}\right] \end{aligned} \tag{9}$$

$$\dot{q} = (1/I_{yy})\left[(I_{zz} - I_{xx})pr + I_{xz}(r^2 - p^2) + \mathcal{M}\right] \tag{10}$$

$$\begin{aligned}\dot{r} &= \left[1\Big| \left(I_{xx}I_{zz} - I_{xz}^2\right)\right]\left[\left(I_{xx}^2 - I_{xx}I_{yy} + I_{xz}^2\right)pq \right. \\ &\quad \left. + (-I_{xx} + I_{yy} - I_{zz})I_{xz}qr + I_{xz}\mathcal{L} + I_{xx}\mathcal{N}\right] \end{aligned} \tag{11}$$

The rotational kinematics are

$$\dot{\phi} = p + (q \sin\phi + r \cos\phi)\tan\theta \tag{12}$$

$$\dot{\theta} = q \cos\phi - r \sin\phi \tag{13}$$

$$\dot{\psi} = (q \sin\phi + r \cos\phi)\sec\theta \tag{14}$$

The engine dynamics are

$$\dot{\xi} = (1/\tau)(\xi_t - \xi) \tag{15}$$

The preceding equations are based on the following assumptions: 1) The wind flow is steady. 2) The Earth is flat and nonrotating. 3) The aircraft weight is constant. The thrust T is assumed to have a fixed inclination δ relative to the zero-lift axis, but the thrust vector remains in the aircraft plane of symmetry. The maximum thrust is assumed to be a function of airspeed only, that is, the thrust, as a function of airspeed and throttle response, is

$$T = \xi\left(T_0 + T_1 V + T_2 V^2\right) \tag{16}$$

The aerodynamic forces and their coefficients are

$$D = \tfrac{1}{2}\rho V^2 \mathcal{S} C_D \tag{17}$$

$$S = \tfrac{1}{2}\rho V^2 \mathcal{S} C_S \tag{18}$$

$$L = \tfrac{1}{2}\rho V^2 \mathcal{S} C_L \tag{19}$$

where[20]

$$C_D = C_{D_0} + C_{D_\alpha}\alpha \tag{20}$$

$$C_S = C_{S_\beta}\beta + C_{S_{\delta_r}}\delta_r \tag{21}$$

$$C_L = C_{L_0} + C_{L_\alpha}\alpha + C_{L_q}(\bar{c}/2V)q_{\text{rel}} + C_{L_{\delta_e}}\delta_e \tag{22}$$

The aerodynamic moments and their coefficients are

$$\mathcal{L} = \tfrac{1}{2}\rho V^2 \mathcal{S} b C_{\mathcal{L}} \tag{23}$$

$$\mathcal{M} = \tfrac{1}{2}\rho V^2 \mathcal{S} \bar{c} C_{\mathcal{M}} + T\Delta z \tag{24}$$

$$\mathcal{N} = \tfrac{1}{2}\rho V^2 \mathcal{S} b C_{\mathcal{N}} \tag{25}$$

where[20]

$$C_{\mathcal{L}} = C_{\mathcal{L}_0} + C_{\mathcal{L}_{\delta_a}}\delta_a + C_{\mathcal{L}_{\delta_r}}\delta_r + C_{\mathcal{L}_\beta}\beta + C_{\mathcal{L}_p}(b/2V)p_{\text{rel}} + C_{\mathcal{L}_r}(b/2V)r_{\text{rel}} \tag{26}$$

$$C_{\mathcal{M}} = C_{\mathcal{M}_\alpha}\alpha + C_{\mathcal{M}_{\delta_e}}\delta_e + C_{\mathcal{M}_q}(\bar{c}/2V)q_{\text{rel}} \tag{27}$$

$$C_{\mathcal{N}} = C_{\mathcal{N}_0} + C_{\mathcal{N}_{\delta_a}}\delta_a + C_{\mathcal{N}_{\delta_r}}\delta_r + C_{\mathcal{N}_\beta}\beta + C_{\mathcal{N}_p}(b/2V)p_{\text{rel}} + C_{\mathcal{N}_r}(b/2V)r_{\text{rel}} \tag{28}$$

Note that the effect of thrust on pitching moment is taken into account. Also note that the stability derivatives with respect to rotational velocities are multiplied by p_{rel}, q_{rel}, and r_{rel}. This is because the linear expansion of the aerodynamic coefficients is based on values of angular rotation relative to the atmosphere.[18,19] Thus, we must use the rotational velocity of the aircraft relative to the atmosphere. Keeping in mind that p, q, and r are written in body frame, the components, in body frame, of the aircraft's rotational velocity relative to the atmosphere are

$$\begin{bmatrix} p_{\text{rel}} \\ q_{\text{rel}} \\ r_{\text{rel}} \end{bmatrix} = \begin{bmatrix} p \\ q \\ r \end{bmatrix} - R(\psi, \theta, \phi)\begin{bmatrix} \dfrac{\partial W_z}{\partial y} - \dfrac{\partial W_y}{\partial z} \\ \dfrac{\partial W_x}{\partial z} - \dfrac{\partial W_z}{\partial x} \\ \dfrac{\partial W_y}{\partial x} - \dfrac{\partial W_x}{\partial y} \end{bmatrix} \tag{29}$$

In the mathematical model the control variables are ξ_t, δ_a, δ_e, and δ_r. They are constrained by

$$0 < \xi_t \le 1, \qquad -20 \le \delta_i \le 20 \text{ deg}, \qquad i = a, e, r \tag{30}$$

From Ref. 21, the 1-g stall speed of a large airliner jet with weight of 564,000 lb and 30-deg flap setting (gear down) is 60.8 m/s. If airspeed drops to the stall speed while angle of attack α is greater than $\alpha_{\max}$ (which is 17.2 deg),[4,10] the aircraft is assumed to stall. Because of the turbulence, there might be instantaneous jumps in angle of attack and airspeed. Thus, the decision on whether the aircraft is stalled is based on the low-frequency components of angle of attack and airspeed that are obtained through low-pass filtering.

The microburst model[10,11] used herein is axisymmetric, three-dimensional, and stationary. The induced radial and vertical wind velocities at any point in three-dimensional space can be computed through the following relations:

$$W_r = f_r \cdot \left(\frac{100}{[(r - D/2)/200]^2 + 10} - \frac{100}{[(r + D/2)/200]^2 + 10}\right) \tag{31}$$

$$W_h = -f_h \cdot \left(\frac{0.4h}{(r/400)^4 + 10}\right) \tag{32}$$

where

$$r = \sqrt{(x - x_c)^2 + (y - y_c)^2} \tag{33}$$

Using polar coordinates, the horizontal wind components W_x and W_y can be readily related to the radial wind component W_r:

$$W_x = \cos\psi_w W_r(r), \qquad W_y = \sin\psi_w W_r(r) \tag{34}$$

Stochastic turbulence is superimposed on the deterministic wind components of Eqs. (32) and (34). Turbulence is modeled using the Dryden power spectral density (PSD) function; specifically, the PSD functions of the translational turbulence components in body-fixed frame are[22]

$$\Phi_{u_g}(w) = \frac{2\sigma_{u_g}^2 L_{u_g}}{V\pi}\frac{1}{\left\{1 + \left(L_{u_g}\middle| V\right)^2 w^2\right\}} \tag{35}$$

$$\Phi_i(w) = \frac{2\sigma_i^2 L_i}{V\pi}\frac{1 + 3(L_i/V)^2 w^2}{\left\{1 + (L_i/V)^2 w^2\right\}^2}, \qquad (i = v_g, w_g) \tag{36}$$

The intensity of the w component of turbulence in the body-fixed frame, σ_{w_g}, is chosen to be 4, which corresponds to a severe storm. The intensities of the other components are computed using the assumption that the intensities of the three translational components of turbulence are isotropic. The scale lengths of turbulence are functions of altitude.[22] The coloring filters needed to generate the appropriate spectral densities for the translational turbulence velocities in a body-fixed frame are also given in Ref. 22. In this microburst model with turbulence, we assume that turbulence and microburst windshear can be modeled independently. Experimental evidence suggests that turbulence length scales increase through a microburst and, in some unknown manner, depend on microburst size and strength.[23] Such a functional dependence between turbulence and microburst parameters will result in a nonstationary and non-Gaussian wind process description.[14] This functional dependence is neglected in this study.

The specific energy E is defined as follows:

$$E = h + V^2/2g \tag{37}$$

An important characteristic parameter used in the evaluation of windshear performance is the F factor.[4,10] Differentiating Eq. (37)

and substituting $\dot{V}$ and $\dot{h}$ from Eqs. (1) and (8) and rearranging, we obtain

$$\dot{E} = V\{[T\cos(\alpha+\delta)\cos\beta - D]/W - (1/g)[er(1,1)\dot{W}_x + er(1,2)\dot{W}_y + er(1,3)\dot{W}_z] + \dot{W}_h/V\} \tag{38}$$

The first term is recognizable as the airplane's available excess thrust-to-weight ratio. The last four terms describe the effect of windshear on the airplane's energy state[24] or potential climb rate. They may be combined into a single scalar quantity, called the F factor, as follows:

$$F = (1/g)[er(1,1)\dot{W}_x + er(1,2)\dot{W}_y + er(1,3)\dot{W}_z] - \dot{W}_h/V \tag{39}$$

The effect of windshear on airplane performance is, thus, expressed as an effective reduction in available specific excess thrust-to-weight ratio due to horizontal and vertical shears and downdrafts.[24] Note that positive values of the F factor indicate a performance-decreasing situation.

Escape Strategies and Controllers

As the aircraft, guided by the landing controller, is descending, the F factor is monitored using data obtained from a reactive detection system. Once the F factor exceeds the threshold value,[11] which is 0.04, the landing is aborted, and an escape maneuver is immediately initiated. In this study only the reactive detection case is considered, that is, the F factor is computed from data taken from the environment where the aircraft is flying, but not ahead of the aircraft on the flight path (which is the forward-looking detection case[25]). In real-time microburst encounters, because the F factor measurement is contaminated by turbulence, the F factor should be filtered before it is used in an escape decision. Although this process of filtering may delay the escape maneuver initiation, no effort is made here to study the effect of this delay on escape performance, and this issue is left as an item of future work. Instead, only the deterministic components of wind velocity are used in F-factor computation. In the literature, there are many studies dealing with real-time F-factor estimation.[14,15,24–28]

There are three guidance strategies for microburst escape maneuver analyzed in this study:

1) The first strategy is pitch guidance: Once the escape maneuver is initiated, a 15-deg target pitch angle is commanded and maintained throughout the microburst as long as the angle of attack is less than its maximum allowed limit $\alpha_{\max}$. This strategy is recommended in the Windshear Training Aid[3] by the FAA.

2) The second strategy is dive guidance: The escape maneuver is initiated by commanding a 0-deg target pitch angle that is maintained until the altitude drops to the commanded altitude h_c. Once the altitude becomes lower than h_c, a 15-deg pitch angle is commanded for the remainder of the escape maneuver. These 0- and 15-deg pitch angles are maintained if the angle of attack is less than $\alpha_{\max}$. Dive guidance is one of the candidate escape maneuvers in the Windshear Training Aid,[3] for which no specific recommendation is made, although some other candidates are not recommended. Also note that pitch guidance is a special case of dive guidance; indeed dive guidance becomes pitch guidance if the commanded altitude is chosen as the altitude where the escape maneuver is initiated.

3) The third strategy is altitude guidance (h guidance): This guidance strategy flies the aircraft at a constant recovery altitude in the high-shear region of the microburst. It has two consecutive modes. In the altitude-guidance mode, it directs the aircraft to the commanded altitude h_c and keeps it there. Then, in the climbing mode, it commands a 15-deg pitch angle to move the aircraft up from its recovery altitude. Here, a switch from altitude to climbing mode is triggered as soon as the energy drain stops, that is, when $\dot{E}=0$. In the simulations, $\dot{E}$, contaminated by turbulence, is passed through a low-pass filter before being used for a switching decision.

The following are common to all three escape maneuvers: 1) full thrust is commanded, that is, $\xi_t = 1$; 2) a 0-deg bank angle is commanded to keep the wings level during the escape maneuver; 3) a 0-deg side-slip angle is commanded; and 4) one of the three escape guidance strategies is employed as long as the angle of attack is

$$-0.5\alpha_{\max} \le \alpha \le 0.9\alpha_{\max} \tag{40}$$

Although we put a lower limit on the angle of attack, the simulation experiments have shown that it never becomes too small in any stage of an escape maneuver. The reasons for imposing a constraint on the angle of attack are that we model the pilot action in response to the stick shaker, as recommended by the FAA,[3] and that we want the flight to stay in the limits of fidelity of the mathematical model used in this study. If the angle of attack goes out of the interval (40), an additional pitch-up or pitch-down command is given to return the angle of attack in the permissible interval. Note that despite this stall prevention maneuver, stall may still occur if the angle of attack exceeds $\alpha_{\max}$ and the airspeed is below the stall speed.

To implement the preceding guidance strategies and control actions, we have designed several controllers, as follows:

1) The first controller is the roll angle controller. This is a proportional–integral–derivative (PID) controller that computes aileron deflection δ_a to track a 0-deg bank angle:

$$\delta_a = K_{p_\phi}\phi + K_{d_\phi}\dot{\phi} + K_{i_\phi}\int_0^t \phi\,\mathrm{d}\tau \tag{41}$$

where K_{p_ϕ}, K_{d_ϕ}, and K_{i_ϕ} are the gains.

2) The second controller is the side slip angle controller. This is also a PID controller used to keep the side slip angle at 0 deg by using the rudder:

$$\delta_r = K_{p_\beta}\beta + K_{d_\beta}\dot{\beta} + K_{i_\beta}\int_0^t \beta\,\mathrm{d}\tau \tag{42}$$

where K_{p_β}, K_{d_β}, and K_{i_β} are the gains.

3) The third controller is the pitch angle controller. This controller is used to track a commanded pitch angle θ_c by using the elevator. The nonlinear dynamic inversion (NDI) technique is used to design this controller. The control law for the elevator deflection is

$$\delta_e = \left(1 \middle| \; f_{\theta_e}\right)\left(u_\theta - f_{\theta_0}\right) \tag{43}$$

where

$$u_\theta = \ddot{\theta}_c - K_{\theta_1}(\dot{\theta}-\dot{\theta}_c) - K_{\theta_2}(\theta-\theta_c)$$

$$f_{\theta_e} = (\cos\phi/I_{yy})f_{\mathcal{M}_e}$$

$$f_{\theta_0} = (\cos\phi/I_{yy})\left[(I_{zz}-I_{xx})pr + I_{xz}(r^2-p^2) + f_{\mathcal{M}_0}\right] - (\sin\phi/\Delta_1)(\Delta_2 pq + \Delta_3 qr + I_{xz}\mathcal{L} + I_{xx}\mathcal{N}) - (q\sin\phi + r\cos\phi)[p + (q\sin\phi + r\cos\phi)\tan\theta]$$

and

$$f_{\mathcal{M}_e} = \tfrac{1}{2}\rho\mathcal{S}\bar{c}V^2 C_{\mathcal{M}_{\delta_e}}$$

$$f_{\mathcal{M}_0} = \tfrac{1}{2}\rho\mathcal{S}\bar{c}V^2\left[C_{\mathcal{M}_\alpha}\alpha + C_{\mathcal{M}_q}(c/2V)q_{\mathrm{ref}}\right] + \Delta zT$$

$$\Delta_1 = I_{xx}I_{zz} - I_{xz}^2, \qquad \Delta_2 = I_{xx}^2 - I_{xx}I_{yy} + I_{xz}^2$$

$$\Delta_3 = I_{xz}(-I_{xx} + I_{yy} - I_{zz})$$

For simplicity, and because air vorticity is difficult to measure, we use, in the computation of the control law in Eq. (43), p, q, and r instead of p_{rel}, q_{rel}, and r_{rel}, respectively. Because we use the NDI technique, the designed controller guarantees that the pitch dynamics will behave like the following second-order system:

$$(\ddot{\theta}-\ddot{\theta}_c) + K_{\theta_1}(\dot{\theta}-\dot{\theta}_c) + K_{\theta_2}(\theta-\theta_c) = 0 \tag{44}$$

as long as δ_e does not saturate.

4) The fourth controller is the stall prevention controller. As explained earlier, this controller takes a counteraction to return the angle of attack within the permissible interval (40) by changing elevator deflection δ_e:

$$\delta_e = K_{\mathrm{dz}} f_{\mathrm{dz}}(\alpha) \tag{45}$$

where K_{dz} is a constant and f_{dz} is a so-called dead-zone nonlinearity

$$f_{\mathrm{dz}}(\alpha) = \begin{cases} \alpha + \alpha_{\mathrm{lower}}, & \text{for} \quad \alpha < \alpha_{\mathrm{lower}} \\ 0, & \text{for} \quad \alpha_{\mathrm{lower}} < \alpha < \alpha_{\mathrm{upper}} \\ \alpha - \alpha_{\mathrm{upper}}, & \text{for} \quad \alpha > \alpha_{\mathrm{upper}} \end{cases} \tag{46}$$

where $\alpha_{\mathrm{lower}} = -0.5\alpha_{\max}$ and $\alpha_{\mathrm{upper}} = 0.9\alpha_{\max}$.

Note that the elevator deflection command is always the sum of the elevator deflections computed by the pitch angle and stall prevention controllers. The dead-zone nonlinearity ensures that only the pitch angle controller is active when the angle of attack is within the permissible interval.

5) The fifth controller is the altitude controller. This controller gives the commanded pitch angle θ_c that takes the aircraft to the commanded altitude h_c and keeps it there. The angle θ_c is computed as follows:

$$\dot{\theta}_c + K_{u_1}\theta_c = K_{u_0} u_c \tag{47}$$

where

$$u_c = K_{p_h}\Delta h + K_{d_h}\Delta\dot{h} + K_{i_h}\int_0^t \Delta h \, \mathrm{d}\tau \tag{48}$$

and K_{p_h}, K_{d_h}, K_{i_h}, K_{u_0}, and K_{u_1} are the gains, and $\Delta h = h_c - h$.

The preceding controllers are used in combination in each escape guidance strategy. The roll angle, side slip angle, pitch angle, and stall prevention controllers are always used in all of the three escape maneuvers. In pitch guidance, $\theta_c = 15$ deg throughout the escape maneuver. In dive guidance, $\theta_c = 0$ deg until h_c is reached, then $\theta_c = 15$ deg for the rest of the escape maneuver. In altitude guidance, the altitude controller is used to compute θ_c, which is fed back into the pitch angle controller until the energy drain stops, that is, $\dot{E} = 0$, then $\theta_c = 15$ deg is commanded to move the aircraft up from the recovery altitude h_c.

Sample Analysis Approach

The simulations were performed with pitch, dive, and altitude guidance of various commanded altitudes in the presence of turbulence. Typical results are presented in Figs. 1–4. The microburst parameters chosen in this section are specified in the title of each figure and are the same as the ones in Refs. 10 and 11.

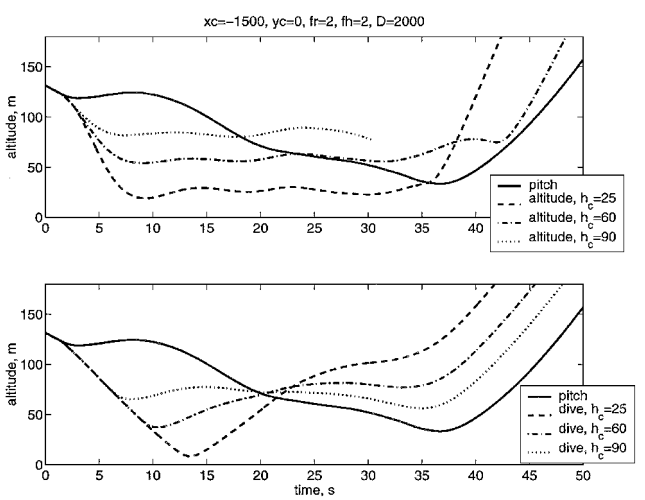

Fig. 1 Typical samples of time histories of altitude in different scenarios.

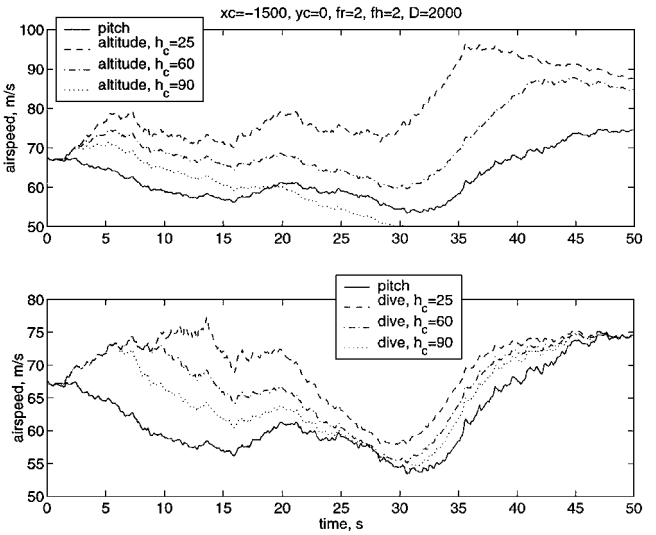

Fig. 2 Typical samples of time histories of airspeed in different scenarios.

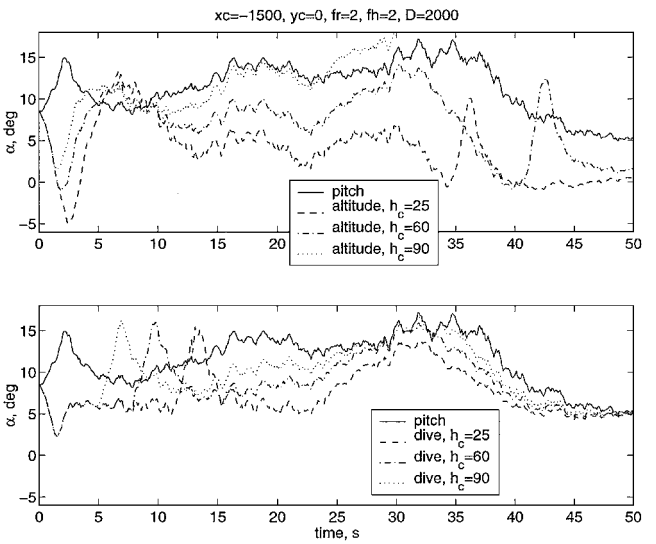

Fig. 3 Typical samples of time histories of angle of attack in different scenarios.

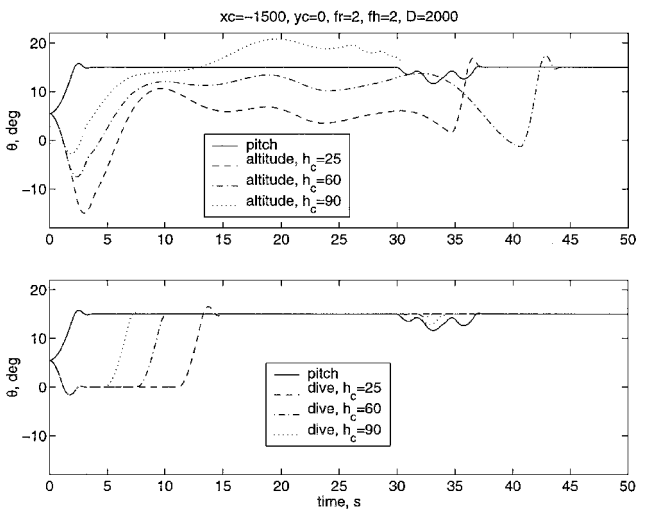

Fig. 4 Typical samples of time histories of pitch angle in different scenarios.

As can be seen in Fig. 1, in this severe microburst, the highest minimum altitude reached during the escape maneuver is obtained with h guidance of about $h_c = 50$ m commanded altitude. Also note that in the case of h guidance with low commanded altitude (in this case lower than 50 m), the minimum altitude is near the commanded altitude. If high altitude is commanded (e.g., 90 m in this case), h guidance may cause the aircraft to stall despite the stall prevention controller. Because our study does not consider post-stall recovery, the simulation is stopped. The dive-guidance trajectories have two minima: one right after 15-deg pitch angle is commanded (i.e., after h_c for dive guidance is reached) and one later in the tailwind region of the microburst. The first minimum is always lower than the commanded altitude. This is because with 0-deg pitch angle, the aircraft has a negative climb rate. Thus, once a 15-deg pitch angle is commanded at h_c, it takes some time first to increase the pitch angle to 15 deg and then to stop descending and start gaining altitude. As Fig. 1 suggests, for low commanded altitude, dive guidance gives the lowest minimum right after the commanded altitude, but for high commanded altitude, the second minimum is lower. This is because the attempt to climb is initiated before enough airspeed is gained and also because a higher commanded altitude exposes the aircraft to stronger downdraft. Figure 1 suggests that there is not as much authority on minimum altitude with pitch and dive guidance as with h guidance of low commanded altitude.

Figure 2 shows that h guidance with high commanded altitude causes stall due to low airspeed and very high angle of attack (also see Fig. 3). Like in Refs. 11 and 15, Fig. 2 shows that with h and dive guidance, altitude is initially traded for airspeed, to fly the aircraft with relatively high airspeed and to position it in a region of relatively low downdraft. Another observation from Fig. 2 is that lower commanded altitude, when dive guidance is used, does not result in a significant airspeed gain in the tailwind region, whereas h guidance with lower commanded altitude gives rise to significantly higher airspeed throughout the whole microburst. In comparison to pitch guidance, dive guidance always results in higher airspeed. However, for h guidance, high commanded altitudes cause low airspeeds, even so low as to cause stall.

Figure 3 suggests that, as the commanded altitude is reduced, the aircraft most of the time flies with lower angle of attack in both h and dive guidance. Exceptions occur at the time of switching between controllers. Flight with lower angle of attack is safer in the sense that it is less likely to turn on the stall prevention controller. Note that during the stall prevention maneuver, a significant altitude drop may occur, and the stall prevention maneuver might not work if the high angle of attack is accompanied with a very low airspeed. Regarding h guidance, during the initial descent to the commanded altitude, the aircraft flies with very low angle of attack, even negative if the commanded altitude is low, for example, $h_c = 25$. If the commanded altitude is very high, for example, $h_c = 90$ in h guidance, the aircraft flies with very high angle of attack, even higher than that of pitch guidance, and runs into stall because the aircraft has not gained enough airspeed. Regarding dive guidance, the angle of attack is always lower than that of pitch guidance except during the switching from a 0- to a 15-deg commanded pitch angle. If the angle of attack time histories for h and dive guidance are compared, it can be seen that with lower commanded altitude, the drop in the angle of attack in h guidance is larger.

How the pitch angle varies can be seen in Fig. 4. With h guidance, the aircraft flies with negative pitch angle during the initial descent to the commanded altitude. Additionally, with lower commanded altitude, the aircraft flies with lower pitch angle through the high-shear region of the microburst. Around the time 35 s, the stall prevention controller, in the case of pitch guidance and dive guidance with high h_c, becomes active to reduce the pitch angle because the angle of attack becomes too high. Also note that h guidance with $h_c = 90$, which causes stall, flies the aircraft with very high pitch angle.

Although the plots are not shown here, the bank angle controller works satisfactorily. There is no danger due to the rolling motion of the aircraft because the bank angle is successfully kept around 0 deg.

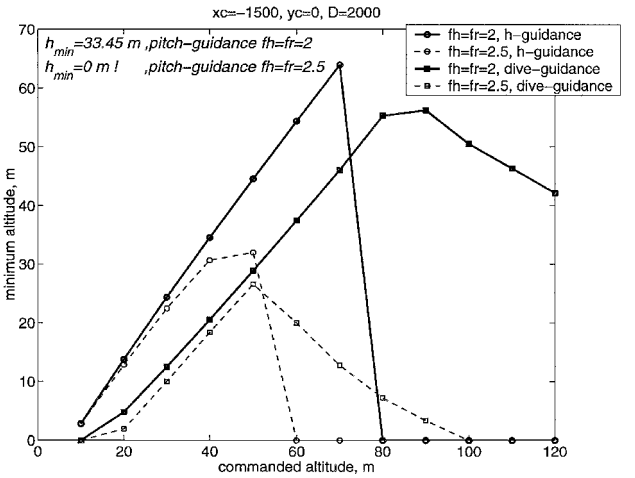

Fig. 5 Minimum altitude vs h_c for different scenarios and microbursts.

Figure 5 plots minimum altitude vs commanded altitude for two different microburst cases. The plots show that for both cases, the maximum minimum altitude is achieved with h guidance. For altitudes higher than the maximum minimum altitudes, h guidance runs the aircraft into stall. Note that in the first microburst case ($f_h = f_r = 2$) pitch guidance results in $h_{\min} = 33.45$ m and that in the second case ($f_h = f_r = 2.5$) the aircraft with pitch guidance crashes. When we compare the minimum altitude curves of the two microburst cases for each strategy, the difference between the curves of h guidance decreases as the commanded altitude decreases for $h_c < 50$ m, but there is a constant difference between the curves of dive guidance. This suggests that h guidance is relatively robust against changes in microburst strength. Even though the aircraft with pitch guidance recovers from the first microburst safely, when the microburst becomes a little stronger pitch guidance causes the aircraft to crash. However, with low commanded altitude h and dive guidance escape both microbursts. Note that dive guidance with $h_c = 10$ m causes ground contact in both microburst cases. Additionally, h guidance with low commanded altitude results in almost the same minimum altitude regardless of the microburst strength.

Statistical Approach

The preceding sections have suggested that once the escape maneuver is initiated, descending to a lower altitude may have certain advantages. We now analyze the sensitivity of this conclusion with respect to variations in microburst size, strength, and location, in the presence of turbulence, using the Monte Carlo method.[29–33] Here, the only data is the statistical distribution of the microburst parameters, and the comparison between different strategies is based on scalar performance measures: the likelihood of survival and the likelihood of descending lower than a given altitude. The Monte Carlo simulation is carried out to obtain a sample of a certain random variable (the minimum altitude) and to estimate, by using this sample, the probability of having minimum altitude less than a given value and the probability of crash.

The minimum altitude $h_{\min}$ depends on the initial conditions at which the aircraft enters the microburst, the parameters of the microburst, turbulence, and the guidance strategy. Hence,

$$h_{\min} = h_{\min}(z_0, \boldsymbol{\theta}, \boldsymbol{K}) \tag{49}$$

Assume that z_0 and $\boldsymbol{K}$ are given and that $\boldsymbol{\theta}$ is a continuous random vector with a given joint probability density function $\boldsymbol{f}_\theta(\boldsymbol{\theta})$. Because $h_{\min}(z_0, \boldsymbol{\theta}, \boldsymbol{K})$ is a function of a random vector, it is also a random variable. Thus, we can define its probability distribution function

$$F_{h_{\min}}(h) = \text{Probability}(h_{\min} \leq h) \tag{50}$$

which tells us the probability of having $h_{\min}$ less than or equal to h. This probability or the probability distribution function of $h_{\min}$ can be computed from

$$F_{h_{\min}}(h) = Pr(h_{\min} \leq h) = \int_{D_\theta} I(\boldsymbol{\theta}, \boldsymbol{K}, h) \boldsymbol{f}_\theta(\boldsymbol{\theta})\, \mathrm{d}\boldsymbol{\theta} \tag{51}$$

where $I(\boldsymbol{\theta}, \boldsymbol{K}, h)$ is the indicator function defined as

$$I(\boldsymbol{\theta}, \boldsymbol{K}, h) = \begin{cases} 1 & \text{when} \quad h_{\min} \leq h \\ 0 & \text{otherwise} \end{cases} \tag{52}$$

Note that

$$F_{h_{\min}}(0) = Pr(h_{\min} \leq 0) \tag{53}$$

is the probability of crash. Also note that because, by definition, maneuvers that run the aircraft into stall are not safe, minimum altitudes in those maneuvers are taken to be zero.

Let $\boldsymbol{\theta}_1, \boldsymbol{\theta}_2, \ldots, \boldsymbol{\theta}_m$ be the outcomes of m independent and identically distributed continuous random vectors, $\boldsymbol{\Theta}_1, \boldsymbol{\Theta}_2, \ldots, \boldsymbol{\Theta}_m$ that take values in D_θ and have probability density function $\boldsymbol{f}_\theta$. The Monte Carlo estimate of the probability distribution function of $h_{\min}$ in Eq. (51) is then simply the frequency of occurrence of the event $h_{\min} \leq h$, over the sample $\boldsymbol{\theta}_1, \boldsymbol{\theta}_2, \ldots, \boldsymbol{\theta}_m$, given by

$$\widehat{Pr}(h_{\min} \leq h) = \frac{1}{m} \sum_{i=1}^{m} I(\boldsymbol{\theta}_i, \boldsymbol{K}, h) \tag{54}$$

The remarkable feature of the Monte Carlo method is that the quality and computational burden of the estimate in Eq. (54), in probabilistic sense, are independent of the dimensionality of the problem.[29–33]

In this paper, the microburst parameters and turbulence vector is

$$\boldsymbol{\theta} = [f_r, f_h, D, x_c, y_c, u_g(\cdot), v_g(\cdot), w_g(\cdot)]^T \tag{55}$$

where $(\cdot)$ indicates that we consider discretized time histories, and the first five components of $\boldsymbol{\theta}$ are independent. In this study, the marginal density functions f_{f_r} and f_{f_h} are assumed to be Rayleigh density functions [the Rayleigh density functions are utilized to fit the statistical data from the Joint Airport Weather Studies (JAWS)[5]], and f_D, f_{x_c}, and f_{y_c} are uniform probability density functions. The statistical properties of $u_g(\cdot)$, and $v_g(\cdot)$, and $w_g(\cdot)$ are defined from Eqs. (35) and (36), respectively.

The first five elements of $\boldsymbol{f}_\theta$ are chosen such that their expected values are equal to the nominal values used in Refs. 10 and 11:

$$E[f_r, f_h, D, x_c, y_c] = [2, 2, 2000, -1500, 0] \tag{56}$$

Thus, the probability density functions of f_r and f_h have the form

$$f_{f_r}(\theta) = f_{f_h}(\theta) = (\theta/\sigma^2) e^{-(\theta^2/2\sigma^2)} u(\theta), \qquad (\sigma > 0) \tag{57}$$

where $u(\theta)$ is the unit step, that is, $u(\theta) = 1$ for $\theta \geq 0$ and $u(\theta) = 0$ for $\theta < 0$.

The probability density function of D is

$$f_D(\theta) = \begin{cases} \frac{1}{100}, & 1950 \leq \theta \leq 2050 \\ 0, & \text{otherwise} \end{cases} \tag{58}$$

The probability density function of x_c is

$$f_{x_c}(\theta) = \begin{cases} \frac{1}{500}, & -1750 \leq \theta \leq -1250 \\ 0, & \text{otherwise} \end{cases} \tag{59}$$

The probability density function of y_c is

$$f_{y_c}(\theta) = \begin{cases} \frac{1}{200}, & -100 \leq \theta \leq 100 \\ 0, & \text{otherwise} \end{cases} \tag{60}$$

Note that in Ref. 5, the parameters defining the intensity of the microburst are also modeled with Rayleigh density functions, and those defining the geometry of the microburst are also modeled with uniform density functions.

The gain vector $\boldsymbol{K}$ for the pitch-guidance controller is assumed to be fixed and for h and dive guidance, the gain vector is

$$\boldsymbol{K} = [h_c] \tag{61}$$

All of the other control parameters have fixed values and, for h guidance, are the same as in Refs. 10 and 11.

Because we use a Monte Carlo simulation to estimate the probability of crash, we must assess the quality of this estimate. For problems of a statistical nature such as the problem at hand, the quality of an estimate is often evaluated with confidence intervals. By confidence interval, we mean a statement of the form

$$Pr(L \leq R \leq U) \geq 1 - \delta \tag{62}$$

where $\delta \in (0, 1)$ are the confidence parameters, and L and U represent lower and upper bounds of the confidence interval, respectively, for the unknown, R. The confidence interval allows us to state that given the sample $\boldsymbol{\theta}_1, \boldsymbol{\theta}_2, \ldots, \boldsymbol{\theta}_m$, the conditional probability of crash lies, with $(1 - \delta) \times 100\%$ certainty, in the interval $[L, U]$. In this study, the approximation methods of Anderson and Burstein in Refs. 31 and 32 are used to compute U and L, respectively. Implementing the aforementioned procedure in flight simulations, the probabilities of crash and the probability distribution function of minimum altitude in microburst encounters, for the three different scenarios, were obtained along with confidence intervals. The probability distribution function of $h_{\min}$ of an aircraft with h and dive guidance was computed for various commanded altitudes. In the computation of confidence intervals the confidence parameter δ was taken to be 0.05, that is, L and U determine 95% confidence intervals. As the number of Monte Carlo trials increases, the confidence interval becomes smaller.[30–33] In this study, no effort was made to tighten the confidence intervals because the goal was only to achieve confidence limits small enough to have conclusive comparisons between the escape strategies.

From Fig. 6, it can be seen that for h guidance with commanded altitude higher than 25 m, the lower the commanded altitude, the lower the probability of crash. For commanded altitudes lower than 25 m, commanding a lower recovery altitude deteriorates the safety of the escape maneuver. Thus, in this particular scenario the minimum probability of crash is achieved when the altitude of 25 m is chosen as the recovery altitude.

When dive guidance is used as escape maneuver, we have a similar pattern of probability of crash vs commanded altitude. That is, we achieve the minimum probability of crash with a commanded altitude of 25 m. However, the reduction in the probability of crash

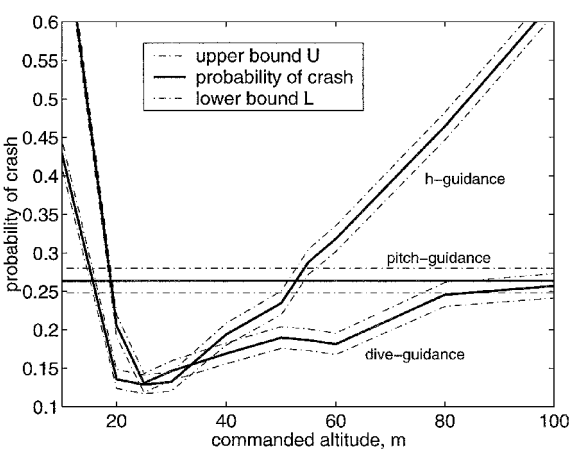

Fig. 6 Probability of crash with confidence intervals, for an aircraft with the three different guidance strategies vs commanded-altitude (this can be adjusted only in the *h*- and dive-guidance strategies).

when dive guidance is used is not as dramatic as in the case of h guidance.

The reduction of the probability of crash in both h guidance and dive guidance happens for two reasons: diving to a lower altitude makes the aircraft gain more airspeed and fly in a region where the downdraft is relatively weak. However, if the aircraft dives too low, that is, lower than 25 m in both h and dive guidances, the turbulence becomes strong enough to affect the aircraft escape path through the microburst. Thus, potential deviations from the aircraft's intended path due to turbulence at low altitude are so significant that flying lower is no longer effective and even increases the probability of crash.

That h guidance with commanded altitude higher than 52 m gives rise to a higher probability of crash than both dive and pitch guidances has two reasons. First, a pilot's commanding the aircraft to remain at a high altitude through the microburst will expose the aircraft to stronger downdraft. On the other hand, if pitch or dive guidance is used, the simulation experiments have shown that the aircraft will fly lower in some part of the escape maneuver (see the Sample Analysis Approach section). Second, remaining at a high altitude may result in a situation where the pilot tries to maintain the altitude while airspeed decreases and angle of attack increases significantly, especially in the tailwind region of the microburst. In this case, the pilot has to pitch the aircraft down to prevent stall. However, every attempt to pitch up will run the aircraft again into stall because airspeed has become too low and angle of attack too high. Thus, a fatal altitude loss may not be prevented.

However, h guidance with a commanded altitude of 10–25 m has a lower probability of crash than that of both dive and pitch guidance. This is because pitch guidance does not exploit the advantages of diving to a low altitude at all. Regarding dive guidance, although the aircraft exploits the advantages of diving, an attempt to ascend before the high-shear region of the microburst is exited puts the aircraft again in a performance-deteriorating situation.

Even if h and dive guidance strategies with low commanded altitude result in lower probability of crash than pitch guidance, one might argue that descending to low altitude is not practical in the sense that it is against a pilot's natural instinct in a critical phase of flight. Because the main concern in a microburst encounter is to avoid a crash, it is instinctive for a pilot to immediately attempt to climb. This makes a pilot see, at first glance, both h and dive guidance strategies as unacceptable, especially with low commanded altitude. On the other hand, pitch guidance will seem perfectly intuitive and acceptable because, once the escape maneuver is initiated, it immediately attempts to increase the altitude.

This reasoning would be valid if pitch guidance did not cause any drop in altitude and resulted in higher minimum altitude than h and dive guidance. However, it can be seen from the time history of altitude (see Fig. 1) that with pitch guidance, after the short initial climb, the aircraft keeps losing altitude throughout the microburst. This loss of altitude causes the aircraft in some cases to have a minimum altitude lower than the minimum altitude when h or dive guidance is used. The pilot, preferring pitch guidance, may end up flying at, or even lower than, the altitude where the pilot would fly if they had used h or dive guidance. Furthermore, losing altitude without any control while attempting to climb may be more unsettling than descending to a desired altitude with full control, even if it is low.

The question is, how likely is it that pitch guidance would yield a minimum altitude lower than that of h and dive guidances? We answer this question with Figs. 7 and 8. The information in Figs. 7 and 8 is more general than that in Fig. 6 in the sense that Fig. 6 shows only $F_{h_{\min}}(h=0)$, whereas Figs. 7 and 8 show $F_{h_{\min}}(h)$ for $-10 \leq h \leq 140$.

Figure 7 shows that with h guidance of commanded altitude 25 m, which gives the lowest probability of crash, the probability of having a minimum altitude less than 15 m is 0.2, much less than that with pitch guidance, 0.3. Thus, with pitch guidance, we have both a higher probability of crash and a higher probability of having minimum altitude less than 15 m. If we choose commanded altitude 40 m, we obtain a lower probability of crash and, at the same time, a lower

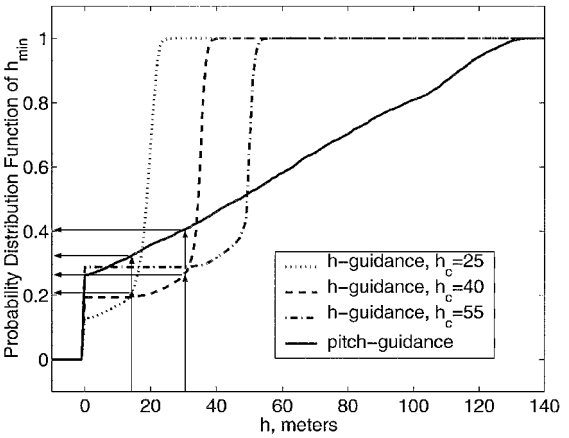

Fig. 7 Probability distribution function of $h_{\min}$ [i.e., $Pr(h_{\min} \leq h)$] of h guidance with various commanded altitudes and of pitch guidance.

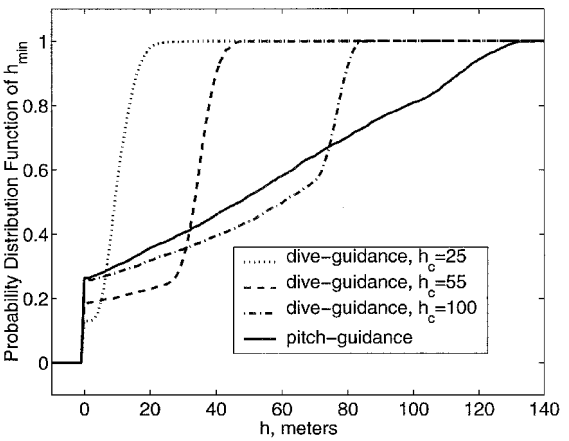

Fig. 8 Probability distribution function of $h_{\min}$ [i.e., $Pr(h_{\min} \leq h)$] of dive guidance with various commanded altitudes and of pitch guidance.

probability of minimum altitude being less than 30 m. Probability distribution function (30) of h guidance with $h_c = 40$ is 0.25 and that of pitch guidance is 0.4. Figure 7 also suggests that h guidance with a commanded altitude about 52 m has a probability of crash equal to that of pitch guidance. Even in this case, h guidance seems more favorable than pitch guidance in the sense that it has a lower probability of having minimum altitude lower than 40 m. The same analysis can be carried out for dive guidance in Fig. 8.

As one can see in Figs. 7 and 8, for altitudes higher than commanded altitudes, the probability distribution functions of minimum altitude in h and dive guidance strategies are greater than that of pitch guidance. Around the commanded altitude, the probability distribution functions of minimum altitude in h and dive guidance strategies have a very sharp increase to 1. That means that, with h- and dive-guidance strategies, the minimum altitude is always equal to or less than the commanded altitude. This is something we should expect because in h and dive guidance, the aircraft is commanded to go to, or fly at, the commanded altitude.

Conclusions

Three escape strategies for microburst encounters during final landing approach have been compared: pitch guidance, dive guidance, and altitude guidance. The main difference between pitch guidance and the other two strategies is that pitch guidance immediately attempts to increase altitude at the expense of airspeed, whereas dive and altitude guidances initially trade altitude for airspeed. Two different methods were used to make a conclusive comparison between the three escape strategies. In the sample analysis approach,

typical samples of the time histories of various variables were used to draw a conclusion. In the statistical approach, the probability distribution function of the minimum altitude was estimated using the Monte Carlo method for all of the three guidance strategies. Additionally, an estimate of the probability of crash was computed by the same method for all of the escape strategies as a function of the commanded altitude.

It appears that trading altitude for airspeed in the initial phase of the escape maneuver, with either dive or altitude guidance, reduces the risk of crash: The two comparison methods suggest that altitude and dive guidance with low commanded altitude may give better performance than pitch guidance as long as the commanded altitude is higher than a certain optimal value. By better performance, we mean increased safety and increased robustness. Altitude guidance with low commanded altitude appears the safest in the sense that it yields the lowest probability of crash. It also appears the most robust in the sense that its safety is least sensitive to variations in microburst size, strength, and location. Furthermore, it affords more authority on the minimum altitude reached during the escape maneuver.

By evaluating the probability distribution function of the minimum altitude, we have developed a novel approach to comparing different escape strategies. Here the comparison is based on the probability of minimum altitude being less than a given altitude. This method has shown that, even if pitch guidance is used with the intention of immediately increasing altitude, the minimum altitude reached during the escape maneuver is very likely to be lower than it would be if dive or altitude guidance were used. Thus, with respect to both crash and minimum altitude reached, pitch guidance does not appear to give better performance than the other two strategies.

Although there are a few other studies[11,15,17] that also suggest the advantage of descending, they neglect the rotational dynamics of the aircraft, the effect of turbulence and air vorticity on the escape performance, and the effect of stall prevention on the escape path. Thus, they fail to show that potential deviations from the aircraft's intended path due to turbulence and the rotational dynamics at low altitude are so significant that flying lower is no longer effective and even increases the probability of crash. However, we have shown that even under the effect of turbulence and air vorticity, and despite the delays and deviations due to the rotational dynamics, an initial descent increases the safety of the microburst escape maneuver as long as the commanded altitude is higher than a certain optimal value. We also have extensive experimental evidence that these conclusions are preserved under changes of approach speed, even though the time histories of the aircraft's state variables are changed.

Although we have shown that altitude and dive guidance with low commanded altitude may provide better safety than pitch guidance, note that this conclusion was drawn within the modeling assumptions of this study and in the absence of human factors. Thus, further research is clearly required before practical recommendation of these alternative guidance strategies. If the results are significantly dependent on the statistical properties of the microburst, then it will be necessary to find the most accurate data available and to confirm the statistical analysis with a more accurate microburst model. This analysis seems to be very crucial in determining the optimal commanded altitude. Even if the results suggest that it is safer to descend to an optimal altitude, in the case of less severe microbursts it is generally possible to safely recover with commanded altitudes that are higher than the optimal commanded altitude. Using windshear information from forward-looking and/or reactive detection systems, this could be accomplished by scheduling the commanded altitude or by determining the highest safe altitude to be used as the commanded altitude. Although the candidate escape maneuvers can be implemented by means of the controller, in practice, the pilot, not a controller, is supposed to implement an escape maneuver in real time. Because the control laws are rather intricate for a pilot, the performance of the escape maneuvers should be tested in piloted flight simulators in an actual microburst wind profile obtained during some of the recent accident/incidents to investigate the sensitivity of the escape strategies to human factors.

Acknowledgments

We would like to thank the reviewers for their contributions to improving this paper. Their critical skepticism has led us to substantially refine the models we used. These refinements have added strength to the findings in our initial submission, pointing to the potential benefits of trading altitude for airspeed. We would also like to thank Associate Editor Kenneth J. Holt for his fairness in the review process. In view of the counterintuitive nature of our results, we are providing the software code we used in this study (http://www-personal.engin.umichedu/adogan/research.htm), so that interested readers may validate our conclusions themselves.

References

[1]Fujita, T. T., "DFW Microburst," Satellite and Mesometeorology Research Project, Univ. of Chicago, Chicago, IL, 1986.

[2]Fujita, T. T., "The Downburst," Satellite and Mesometeorology Research Project, Univ. of Chicago, Chicago, IL, 1985.

[3]"Windshear Training Aid," U.S. Dept. of Transportation, Federal Aviation Administration, Washington, DC, 1987.

[4]Miele, A., Wang, T., Melvin, W. W., and Bowles, R. L., "Acceleration, Gamma, and Theta Guidance for Abort Landing in a Windshear," *Journal of Guidance, Control, and Dynamics*, Vol. 12, No. 6, 1989, pp. 815–821.

[5]Krishnakumar, K., and Bailey, J. E., "Inertial Energy Distribution Control for Optimal Windshear Penetration," *Journal of Guidance, Control, and Dynamics*, Vol. 13, No. 6, 1990, pp. 944–951.

[6]Psiaki, M. L., and Stengel, R. F., "Optimal Aircraft Performance During Microburst Encounter," *Journal of Guidance, Control, and Dynamics*, Vol. 14, No. 2, 1991, pp. 440–446.

[7]Mulgund, S. S., and Stengel, R. F., "Optimal Recovery from Microburst Windshear," *Journal of Guidance, Control, and Dynamics*, Vol. 16, No. 6, 1993, pp. 1010–1017.

[8]Mulgund, S. S., and Stengel, R. F., "Target Pitch Angle for the Microburst Escape Maneuver," *Journal of Aircraft*, Vol. 30, No. 6, 1993, pp. 826–832.

[9]Mulgund, S. S., and Stengel, R. F., "Aircraft Flight Control in Windshear Using Sequential Dynamic Inversion," *Journal of Guidance, Control, and Dynamics*, Vol. 18, No. 5, 1995, pp. 1084–1091.

[10]Visser, H. G., "Optimal Lateral-Escape Maneuvers for Microburst Encounters During Final Approach," *Journal of Guidance, Control, and Dynamics*, Vol. 14, No. 6, 1994, pp. 1234–1240.

[11]Visser, H. G., "Lateral Escape Guidance Strategies for Microburst Windshear Encounters," *Journal of Aircraft*, Vol. 34, No. 4, 1997, pp. 514–521.

[12]Leitmann, G., and Pandey, S., "Aircraft Control Under Conditions of Windshear," *Proceedings of the 29th Conference on Decision and Control*, Inst. of Electrical and Electronics Engineers, New York, 1990, pp. 747–752.

[13]Leitmann, G., and Pandey, S., "Aircraft Control for Flight in an Uncertain Environment: Takeoff in Windshear," *Journal of Optimization Theory and Applications*, Vol. 70, No. 1, 1991, pp. 25–55.

[14]Prasanth, R. K., Bailey, J. E., and Krishnakumar, K., "Robust Windshear Stochastic Controller–Estimator," *Journal of Guidance, Control, and Dynamics*, Vol. 15, No. 3, 1992, pp. 679–686.

[15]Zhao, Y., and Bryson, A. E., Jr., "Optimal Paths Through Downbursts," *Journal of Guidance, Control, and Dynamics*, Vol. 13, No. 5, 1990, pp. 813–818.

[16]Avila de Melo, D., and Hansman, R. J., "Analysis of Aircraft Performance During Lateral Maneuvering for Microburst Avoidance," *Journal of Aircraft*, Vol. 28, No. 12, 1991, pp. 837–842.

[17]Dogan, A., and Kabamba, P. T., "Microburst Escape Using Altitude Guidance," *Proceedings of the 37th IEEE Conference on Decision and Control*, Inst. of Electrical and Electronics Engineers, New York, 1998, pp. 4228–4233.

[18]Frost, W., and Bowles, R. L., "Windshear Terms in the Equations of Aircraft Motion," *Journal of Aircraft*, Vol. 21, No. 11, 1984, pp. 866–872.

[19]Brockhaus, R., *Comparison of a Mathematical One-Point Model and a Multi-Point Model of Aircraft Motion in Moving Air*, AGARD-AG-301, Vol. 1, 1990, pp. 3-1–3-17.

[20]Roskam, J., *Airplane Flight Dynamics and Automatic Flight Controls*, DAR Corp., Lawrence, KS, 1995, pp. 543–549.

[21]"Boeing 747-400 Airplane Flight Manual," D6U10001, The Boeing Co., Seattle, WA, Jan. 1989.

[22]Donald McLean, *Automatic Flight Control Systems*, Prentice–Hall, Englewood Cliffs, NJ, 1990, pp. 127–150.

[23]Campbell, C. W., "A Spatial Model of Wind Shear and Turbulence for Flight Simulation," NASA TP-2313, 1984.

[24]Elmore, K. L., Albo, E. D., and Goodrich, R. K., "Estimating Aircraft Performance Loss in Wind Shear from Doppler Radar," *International Conference on Radar Meteorology*, American Meteorological Society, Boston, MA, 1991, pp. 637–675.

[25]Bowles, R. L., "Windshear Detection and Avoidance: Airborne System

Survey," *Proceedings of the 29th Conference on Decision and Control*, Inst. of Electrical and Electronics Engineers, New York, 1990, pp. 708–736.

[26]Hinton, D. A., "Forward-Look Windshear Detection for Microburst Recovery," *Journal of Aircraft*, Vol. 29, No. 1, 1992, pp. 63–66.

[27]Vicroy, D. D., "Assessment of Microburst Models for Downdraft Estimation," *Journal of Aircraft*, Vol. 29, No. 6, 1992, pp. 1043–1048.

[28]Bracalente, E. M., Britt, C. L., and Jones, W. R., "Airborne Doppler Radar Detection of Low-Altitude Windshear," *Journal of Aircraft*, Vol. 27, No. 2, 1990, pp. 151–157.

[29]Kalos, M. H., and Whitlock, P. A., *Monte Carlo Methods, Volume I: Basics*, Wiley, New York, 1986.

[30]Sobolí, I. M., "*A Primer for the Monte Carlo Method*, CRC Press, Boca Raton, FL, 1994.

[31]Anderson, T. W., and Burstein, H., "Approximating the Upper Binomial Confidence Limit," *Journal of American Statistical Association*, Vol. 62, 1967, pp. 857–861.

[32]Anderson, T. W., and Burstein, H., "Approximating the Lower Binomial Confidence Limit," *Journal of American Statistical Association*, Vol. 63, 1968, pp. 1413–1415.

[33]Ray, L. R., and Stengel, R. F., "Application of Stochastic Robustness to Aircraft Control Systems," *Journal of Guidance, Control, and Dynamics*, Vol. 14, No. 6, 1991, pp. 1251–1259.